Nanoscale

Accepted Manuscript

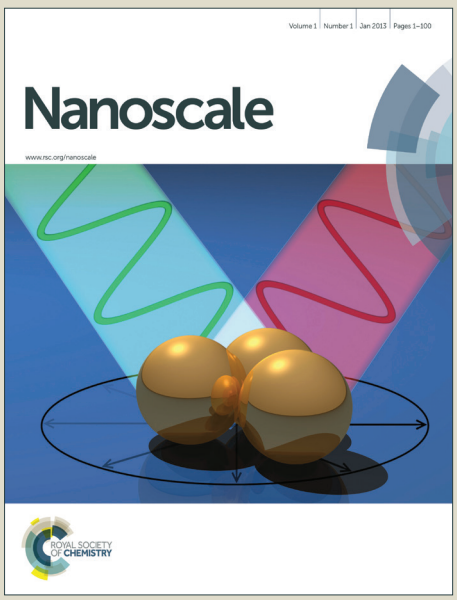

ROYAL SOCIETY OF CHEMISTRY

www.rsc.org/nanoscale

Table of Contents Entry

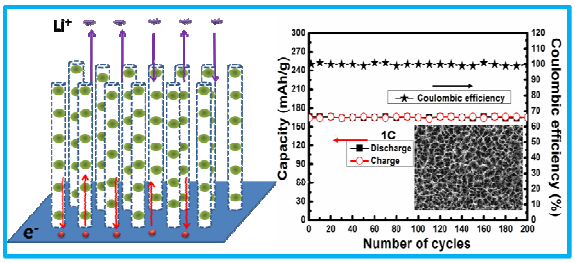

A novel peapod-like C/TiO_2 array with high conductive architecture is designed and fabricated on Ti-substrate for application in high-performance Li-ion batteries.

Self-supported Peapod-Like Mesoporous TiO_2-C Array with Excellent Anode Performance in Lithium-Ion Batteries

*Liang Peng, Huijuan Zhang, Yuanjuan Bai, Yan Zhang, Yu Wang**

The State Key Laboratory of Mechanical Transmissions and the School of Chemistry and Chemical Engineering, Chongqing University 174 Shazheng Street, Shapingba District, Chongqing City, P.R. China, 400044

E-mail: wangy@cqu.edu.cn; prospectwy@gmail.com

Supporting information for this article is available.

Keywords: TiO_2, Carbon, nanotubes array, Lithium-ion batteries

Abstract

Herein, we introduce a novel architectural peapod-like array with TiO_2 nanoparticles encapsulated in graphitized carbon fiber for the first time. The unique peapod-like TiO_2 arrays with high conductivity architectures are designed and fabricated for applying in Li-ion batteries. Since the as-synthesized TiO_2 peapods array is characterized with the large surface area derived from the mesoporous carbon fiber, as well as the high conductivity further enhanced by a thin carbon coating layer, it has showed superior rate capability, high specific capacitances, and excellent cycling stability, e.g. the specific capacity can reach up to 162 mAh/g over 200 cycles. A rational and universal approach to fabricate high-performance TiO_2 peapods array for constructing next-generation Li-ion batteries is demonstrated in this paper. Furthermore, due to the specific of the structure and the versatility of TiO_2, the nanocomposite also can be applied in photochemical catalysis, electronics, biomedicine, gas sensing and so son.

Introduction

With the increasing power and energy demand in applications ranging from next-generation electric vehicles and modern consumer electronics to micro- and nano-electromechanical systems, recent researches have focused on new electrode materials for improving energy storage devices.[1-5] Among all of the various of devices, Li-ion batteries (LIBs) have attracted great attention owing to a number of excellent performances, including higher theoretical capacity, long cycle life, and safety during operation.[6, 7]As far as the current LIBs using graphite anode materials are concerned, the cycle life and rate performance are poor, and the safety issues are serious due to the solid electrolyte interphase film (SEI).[8] As a kind of alternative material to graphitic carbon, the transition -metal oxide such as SnO_2, Co_3O_4, TiO_2, and Fe_2O_3, have been extensively studied as promising anode for high-performance LIBs.[9-12]

In particular, TiO_2 has drawn extensive interest as a potential anode material for LIBs owning to its cycling stability, natural abundance, low cost, and eco-friendliness.[13, 14] However, the practical use of TiO_2 as anode material is greatly limited by both its poor electrical conductivity and low Li-ion diffusivity, which will weaken the charge-discharge property of the LIBs. Moreover, the agglomeration of common anode material, powder or bulk TiO_2, will result in deterioration of rate capability, cyclability, and specific capacity. The major effective ways to improve the utilization of TiO_2 are to reduce the TiO_2 particles to the nanometer range, design and synthesize carbon-coating composites, and dope the electrode materials with other atoms. For example, Zeng and coworkers synthesized the uniform TiO_2@carbon composite nanofibers as anode for enhanced

electrochemical performance.[15] Liu, Hu, et al. fabricated a self-assembled TiO_2-graphene hybrid nanostructures for enhanced Li-ion insertion.[13, 16] Li and coworkers designed and prepared an Ag-modified TiO_2 nanotube as the active anode material to improve electrochemical performance for LIBs.[17] Taking together, the excellent high-performance TiO_2-based electrode materials must be featured with a desired structure of small-sized TiO_2 nanoparticles, a stable framework of samples, and the good electrical conductivity with the help of the conductive additives.

In this paper, we report a facile approach to synthesize a novel TiO_2 nanoparticles@graphitized carbon (TiO_2-C) peapoded fibers array nanostructure. We successfully initiated and developed a mesoporous and sing-crystal TiO_2 fibers array on Ti foil with prepared $H_2Ti_3O_7$ nanotubes array as the template and precursor and coated glucose molecules layer as the carbon sources, which is then converted into the TiO_2 -C peapods array via annealed treatment at 800 ^oC for 6h.[14, 18] The obtained peapod-like nanocomposite has several admirable characters, such as isolation and dispersion of the TiO_2 nanoparticles in the carbon fibers, small size of the peapods down to around 20-30 nm in diameter, and mesoporous and good graphitization of carbon fibers, entirely verified high-performance in LIBs anode, e.g. high specific capacitance (162 mAh/g by galvanostatic charge-discharge at 1C), excellent cycling performance (nearly no capacity loss over 200 cycles), and good rate performance (124 mAh/g at 10 C). Therefore, it is noteworthy that one-dimensional (1D) nanostructure arrays grown directly on a current collector can largely overcome the drawbacks of scattering TiO_2 and exhibit superior electrochemical performance.

Experimental Section

Materials: All materials or reagents were of analytical grade and were used without further purification before used. sodium hydroxide (NaOH, 99.9%, Aldrich), hydrochloric acid (HCl, 37 Wt%, J.T.Baker), titanium foil (0.127 mm (0.005 in.) thick, 99%,Alfa Aesar), D(+)-glucose (Cica-reagent, kanto Chemical), and metallic Li foil (99.9%, Aldrich).

Synthesis of Titanic Acid ($H_2Ti_3O_7$) nanotubes Array.

Prior to the synthesis, Ti foils (2.0×1.0 cm) were rinsed with deionized water and pure ethanol, and acetone (volume rate=1:1:1) for 10 min., and then dried in a nitrogen gas flow. Afterward, the Ti foil was put into a Teflon-lined stainless steel autoclave (50 ml) loaded with 40 mL of 5 M NaOH solution. The Ti foil was against the wall of the autoclave at a certain angel. The autoclave was tightly sealed and left in a preheated electric oven at 180 ^oC for 3h under autogenously pressure and static conditions, and then air-cooled to room temperature. After hydrothermal processing, the sample was washed with DI -water several times and immersed into 0.5 M HCl for 24 h to obtain the $H_2Ti_3O_7$ nanotubes array.

Synthesis of TiO_2-C peapods array nanocomposite.

One Ti foil with $H_2Ti_3O_7$ Nanotubes Array covered tightly tilted against the inner wall of a 50 ml Teflon liner. Then glucose aqueous solution (5mL, 1M) was together with additional D.I.water (35 mL) to form a homogeneous solution after stirring 15 min. The above solution was transferred into the above-mentioned 50 mL Teflon-lined autoclave and sealed tightly. Then the liner was heated in an electric oven at 180 ^oC for 6 h .After heat treatment the liner was cooled down to room temperature, and then the samples were washed for several times using deionized water and pure ethanol. After that, the samples dried in an oven at 60 ^oC overnight to remove the residue water and ethanol. Afterward, the product was annealed at 800 ^oC for 6 h in Ar atmosphere to obtain the final TiO_2-C peapods array.

Materials characterizations.

The TiO_2-C peapods array were characterized by powder X-ray diffraction (Bruker D8 Advance X-ray diffractometer with Cu Kα radiation), Scanning electron microscope(SEM, JEOL, JSM-7800F), transmission electron microscopy (TEM, JEOL, JEM-2100F, 200KV) and field-emission scanning electron microscopy (FESEM; JEOL, EOL, JSM-6700F, 5kV) coupled with an energy dispersive spectrometer (EDS) analyzer, Raman spectroscopy (RENISHAW Invia Raman Microscope, voltage (AC) 100-240 V, power 150 W) and Brunauer – Emmett-Teller surface area measurement (BET, Quantachrome Autosorb-6B surface-area and pore-size analyzer).

Carbon content tests

In a simple method, 300 mg of the composite (TiO_2-C) was scraped off by using a thin knife and further calcined in muffle furnace at 800 ^oC in the air atmosphere. After 10 hours treated, the outside carbon layers were completely burn up and just remain TiO_2 nanoparticles alone. The TiO_2 nanoparticles weight was measured by a Mettler-Toledo analytical balance. Then, the carbon content in the TiO_2-C composite was calculated using this formula: C%= $[W(TiO_2\text{-}C)\text{-}W(TiO_2)]/W(TiO_2\text{-}C)\times 100$ %. Where $W(TiO_2\text{-}C)$ and $W(TiO_2)$ were the weight of primary composite and remain TiO_2 particles, respectively. By this method, the content of carbon is around 6.4 wt.%, thus, its contribution to the capacity is very low.

Electrochemical measurements

Before electrochemical texting, Ti foil was cut into small pieces with size of 0.5×0.5 cm and weighed in a high-precision analytical. The obtained Ti foil as the working electrode. The cells consisted of the as-prepared working electrode, lithium metal used as the counter and reference electrode, and an electrolyte of 1.0 M $LiPF_6$ dissolved in a mixture of EC (ethylene carbonate) and DEC (diethyl carbonate) with the volume ration of 1:1. A Celgard 2400 membrane was used as the cell separator .The cells were constructed in an Ar-filled glove box .The galvanostatic cycling was performed on Neware battery testing system, model 5V 1^{-5}mA, and cyclic voltammetry (CV) was collected using Autolab (AUT71740).The electrochemical impedence measurements were carried out by applying an AC voltage of 5 mV in the frequency from 0.01 Hz to 100 kHz. The specific capacity and current density were calculated based on the mass of the active material in the working electrode. After testing, the tested TiO_2-C peapods array was scraped from Ti foil by knife, and then the Ti foil was cleaned by ultrasonication subsequently and then weighed in the analytical balance again. Through this way, the exact sample mass used for Li-ion battaries texting was available. All the electrochemical measurements were carried out using three-electrode system at ambient temperature.

Results and Discussion

As illustrated in Figure 1, the fabrication process of TiO_2-C peapods array on Ti foil includes four steps. In the first step, Ti foils were rinsed with DI-water, pure ethanol and acetone (volume rate=1:1:1) mixed solution to clean its surface.[19, 20] In the second step, titanic acid ($H_2Ti_3O_7$) nanotubes array was grown on the Ti foil according to hydrothermal and subsequent ion-exchange reaction.[21] In the third step, a polymeric layer derived from the polymerization of glucose at hydrothermal conditions was formed on the surface of $H_2Ti_3O_7$ nanotubes. As an acidic material, $H_2Ti_3O_7$ nanotube has plenty hydroxyl groups or chemically combined H_2O molecules expose on the nanotube surface. With the assistance of hydrogen bonding and H_2O molecules between glucose molecules and $H_2Ti_3O_7$ nanotubes, a polymeric layer source from the polymerization of glucose at hydrothermal conditions was reasonably formed on the surface of $H_2Ti_3O_7$ nanotubes.[7,

[22] In the final step, the polymer-coated nanotubes were subsequently annealed in inert atmosphere, which led to the uniform coating of graphitized carbon layers on the nanotubes surface; meanwhile, the $H_2Ti_3O_7$ nanotubes were *in-situ* converted into TiO_2 nanoparticles encapsulated in the carbon layers. So the final product, the TiO_2-C peapods array was harvested.[23, 24]

Scanning electron microscopy (SEM) was used to evidently disclose the morphology of the $H_2Ti_3O_7$ nanotubes and the TiO_2-C peapods array. In the locally magnified SEM image, as shown in Figure 2a, we could observe that many 1D nanostructures basically aligned together along the outward orientation although some of them are partially inter-crossed. From figure 2(c,d), the locally SEM images, some 1D nanostructures which had a uniform diameter of ~20 nm, could be clearly found. By careful observation, we could easily draw a conclusion that these 1D nanostructures originated from the same starting point and grew along the common direction, which almost was upright to surface of the Ti foil (Figure 2b).[21] Furthermore, it was worthy to note that our samples were closely sticky to the substrate with a length of ~2 μm. No samples would apparently peeled off from the Ti foil though after strong urtrasonication, due to the samples grown directly on the substrate. Their corresponding X-ray diffraction (XRD) patterns indicated that the achieved 1D nanostructures were pure $H_2Ti_3O_7$ (Figure S1) (JCPDS NO.47-0561). Figure 3(a,b) shown typical low-magnification SEM images of the TiO_2-C peapods array on Ti foil, meaning that the morphology and arrayed nanostructure of TiO_2-C peapods array had been preserved in the final samples. High-magnification SEM (Figure c,d) also revealed that many peapod-like nanofibers were aligned together, which matched very well with that of the precursor, $H_2Ti_3O_7$ nanotubes. Because high-energy scanning electron beams accelerated by 15 kV could easily penetrate the thin carbon layer, the encapsulated TiO_2 nanoparticles clearly exhibited and uniformly distributed along the carbon fiber. As shown in Figure 3e, the as-prepared black samples were uniformly distributed and firmly adhered onto the Ti foil. The XRD measurement was also carried out to determine the phases of the final products. Figure 3f shown the typical XRD pattern of TiO_2 (JCPDS No. 21-1272) and their sharpness indicated good crystallinity.[25] The EDS spectrum from SEM, showed in Figure S2, certificates the presence of C, O, Ti. From the SEM and XRD analysis, we could draw a conclusion that the TiO_2-C peapods arrays were pure-phase, single-crystal and the individual peapod-like nanotubes separated from each other.

After the precursor and final peapods array were peeled off the Ti substrate, we could clearly observe the detailed nanostructures of both of them from the transmission electron microscopy (TEM) images (Figure 4). Figure 4a showed a low-magnification TEM image, which revealed that the precursors were composed of 1D hollow nanotubes with a diameter of about 20 nm. Figure 4b showed the high-resolution TEM (HRTEM), these nanotubes exhibited a shell thickness of about 2-4 nm. The lattice spacing of 0.78 nm corresponded to the (200) plan of $H_2Ti_3O_7$.[26] In the typical TEM image (Figure 4c), the peapod-like conformation of the final samples were further demonstrated, where the TiO_2 nanoparticles were aligned within liner carbon fibers, inheriting the nanostructure of precursor. Meanwhile, it could see that the diameter of TiO_2 nanoparticles were about 20-30 nm. Figure 4d, HRTEM analysis, was used to determine the crystal details of the encapsulated TiO_2. The lattice fringes with a spacing of 0.352 nm were belonged to the stable and common observed anatase TiO_2 (101).[27-29] It was interesting to disclose that the orientation of these (101) lattice fringes in a great range is nearly the same, which declares the single crystal microstructure within a single nanoparticle, and correspond to the XRD analysis.

The specific surface areas and pore size distribution of the as-prepared TiO_2-C peapod arrays

were further investigated by nitrogen adsorption-desorption measurements, as shown in Figure 5. From Figure 5a, we can reveal that the curves showed a typical Langmuir type Ⅳ characteristic of a distinct hysteresis loop, meaning the characteristics of a mesoporous material.[30, 31] The porous structure was further confirmed by the Barrett-Joyner-Halenda (BJH) pore size distribution data (Figure 5b). The Brunauer-Emmett-Teller (BET) surface area and the center pore size distribution of the TiO_2-C peapod arrays were 93.6 m^2/g and 3.6 nm, respectively. The TiO_2-C peapod arrays with a large surface area and mesoporous nanostructure which may facilitate the Lithium-ion (Li-ion) and electrons transfer at the electrode/electrolyte interface have potential application in LIBs. The compared Raman spectra of bare TiO_2 and TiO_2-C peapods array were shown in Figure S3**.** The peaks centered at 198, 402 and 632 cm^{-1} were agree with the peaks of TiO_2, while the peaks located at 1348 and 1584 cm^{-1} were attributed to the D and G bands of carbon, respectively.[32-34] In comparison to bare TiO_2, the D and G bands for the TiO_2-C peapod arrays sample means the carbon successfully covered the final products surface. Therefore, based on the results above, we colud further confirm that the TiO_2-C peapods array was made up of single crystalline TiO_2 as energy seed and carbon fiber as protection shell. To our best of knowledge, this was the first report of the directly growth of TiO_2-C peapod arrays on Ti substrate.

Anatase TiO_2 has been wildly researched as the host structure for reversible LIBs. In a TiO_2/Li half-cell, the principal reaction that controls the electrochemical process was as follow:

$$TiO_2 + XLi^+ + Xe^- \leftrightarrow Li_xTiO_2$$

As previous reports, the maximum number of Li^+ that can be inserted is determined to be 0.5, this leads to a theoretical charge capacity of 167.5 mAh/g.[28, 35] Aiming at confirming the excellent performance in LIBs for the designedly synthesized TiO_2-C peapods array, a series of electrochemical measurements have been carried out. Figure 6a shows the description of galvanostatic test with working potential vs. specific capacity from 1st to 50th cycle at a rate of 1C. In figure 6a, we can observe that, all of the charge-discharge curves have a strong tendency to be steady, which matches very well with the cyclic voltammetry (CV) profiles (Figure 6b). It can be seen that the electrode shows a wide voltage plateau at around 1.72 V during the different charge-discharge processes. The plateaus are related to the crystal structure transition with Li insertion into anatase TiO_2.[28, 36] The discharge-capacity of the first cycle was close 230 mAh/g, which was higher than the theoretical capacity for TiO_2 (167.5 mAh/g). As previously reports, it could be due to the irreversible reactions such as the formation of the solid electrolyte interface (SEI).[28, 37-39] Meanwhile, we also can see that from first cycle onward until the fiftieth cycle, the TiO_2-C peapods array displays superior properties in the high specific capacities at a charge-discharge rate of 1C, symbolizes with characteristics of very steady supply source of 164 mAh/g. In Figure 6b, the CV was applied to reveal the electrochemical details when the battery was set to be scanned at 0.5 mV/s within the cutoff-voltage window of 1.0-3.0 V. In agreement with previous reports, two clearly current peaks are seen at 1.72 V (cathodic sweep) and 2.14 V (anodic sweep). The peak at 1.72 V corresponds to the phase transition between tetragonal anatase and orthorhombic $Li_{0.5}TiO_2$ when the insertion coefficient x reaches ~ 0.5. These peaks display no obvious change in amplitude and voltage positions during the 10th cycles, implying the high reversibility of these electrochemical reactions.

In order to confirm the improved rate capability and cyclability, both high rate and long time cycling have been imposed on the TiO_2-C peapods array as shown in Figure 6c. As is display in

Figure 6c, we can see that a very stable capacity of 184 mAh/g (x=0.55) is presented after 40 cycles at a charge/discharge rate of 0.2C. Subsequently, with the charge/discharge rate gradually increased to 1, 2, 5 and 10C for 40 cycles, the corresponding capacities also vary from 164 (x=0.49), 156 (x=0.47), 139 (x=0.41) and 124 (x=0.37) mAh/g, respectively, confirming the excellent rate capability. Then, when the current density is come back to 1C, the specific capacity of 162 (x=0.48) mAh/g can still be reached and the capacity retention was as high as 99%, meaning the enhanced recoverability, stability and cyclability for our sample when texted at very high rate and for a long time running. The result has further verified the synergic effect for the encapsulating nanocomposite in LIBs. In the counting of Coulombic efficiency, the TiO_2-C peapods array possess an value close to 100% within 200 cycles at a current density of 1C (Figure 6d), which further illustrates that the designedly synthesized peapod-like array is a promising superior anode material for the next generation LIBs. Meanwhile, according to the EIS analysis (Figure S4), the TiO_2-C peapods array electrode exhibits very low resistances both in electron-transport and Li-ion diffusion. Furthermore, the temperature-dependent of electrochemical Li storage performance has been texted as well, where the display specific capacity after 200 cycles run at 10C is increased with the experimental temperature changing from 0, 25 and 50 ^{o}C (Figure S5, Supporting Information).[24, 40] Meanwhile, the sample is still characteristic of the excellent stability and cyclability, which is the powerful guarantee to meet the requirement of the next general LIBs.

By analysis of the characteristics of TiO_2-C peapods array nanocomposite, we can reveal the reason why our sample can enhance the properties in electrochemical Li storage. As shown in Figure 7, the hierarchical peapod arrays on Ti foil with unique nanostructure and architecture are presented. Firstly, the graphitic carbon layer self-organizes to a conductive network which contributes to fast charge transfer.[41, 42] Secondly, the carbon layer can prevent the coated TiO_2 nanoparticles from aggregation and agglomeration during charge-discharge process, which is significantly important for the capacity retention of LIBs, especially under high current density and great meaning for the enhancement of rate capability. Thirdly, the interspaces in the carbon fibers between the TiO_2 particles can effectively eliminate possible volume changes during charge-discharge cycling so that the peapod-like architectural integrity is well kept.[22, 43] It is an exciting thing that TiO_2 has a low volume expansion and polarization when charge-discharge cycling relative to other electrode materials, e.g. Sn, S, Si and SnO_2 etc.[44-46] This contributes to the electrolyte fast diffuse and the rapidly exchange of Li-ion, so that improved cyclability and response to increased current densities are highly expected. Fourthly, the mesoporous structure of carbon layers and small size of the TiO_2 peapods with around 20 nm in diameter will effectively promote the electrolyte′s penetration and Li-ion exchange rate for LIBs, which is also the reason to possess the excellent Li storage property for the TiO_2-C peapods array. In the end, the free-standing structure can also contributes to enhancing the kinetics of electron and ion transport in electrodes and the anode materials during charge-discharge process, resulting in excellent electrochemical performance. Collect all of above details, the enhanced electrochemical properties of our sample is reasonably source from the unique peapod-like arrays composite.

Conclusions

A peapod-like arrays composite consisting of TiO_2 particles encapsulated in graphitic carbon fibers has been introduced for the first time. Our sample with the unique nanostructure is a superior anode material in LIBs. The special hierarchical nanostructure combines the fascinating

characters, e.g. single crystal TiO_2 nanoparticles, mesoporous nanostructure and uniformly dispersed TiO_2-C peapods array, and confirm an excellent Li storage performance such as rate capability, superior cyclability and wonderful temperature-dependent effect. All of the enhanced performance is mostly due to the characters of the unique hierarchical structure, including high contact surface area, shortened Li-ion diffusion distance and good structure stability of the arrays. The self-supported TiO_2 anode electrodes without any auxiliary materials are also the shining point for the sample. Furthermore, this research provides an operable model for the design synthesis of the high-performance LIBs for the power flexible electronic devices.

Acknowledgements

This work was financially supported by the Thousand Young Talents Program of the Chinese Central Government (Grant No.0220002102003), National Natural Science Foundation of China (NSFC, Grant No. 21373280,21403019), Beijing National Laboratory for Molecular Sciences (BNLMS) and Hundred Talents Program at Chongqing University (Grant No. 0903005203205).

Supporting Information Available: More SEM, XRD, Raman date are available in the supporting information for this paper.

Reference

1. M. Armand and J. M. Tarascon, *Nature*, 2008, **451**, 652-657.
2. D. Deng, M. G. Kim, J. Y. Lee and J. Cho, *Energy Environ. Sci.*, 2009, **2**, 818-837.
3. S. H. Liu, H. P. Jia, L. Han, J. L. Wang, P. F. Gao, D. D. Xu, J. Yang and S. N. Che, *Adv. Mater.*, 2012, **24**, 3201-3204.
4. J. Chmiola, C. Largeot, P. L. Taberna, P. Simon and Y. Gogotsi, *Science*, 2010, **328**, 480-483.
5. Y. W. Zhu, S. Murali, M. D. Stoller, K. J. Ganesh, W. W. Cai, P. J. Ferreira, A. Pirkle, R. M. Wallace, K. A. Cychosz, M. Thommes, D. Su, E. A. Stach and R. S. Ruoff, *Science*, 2011, **332**, 1537-1541.
6. L. F. Shen, B. Ding, P. Nie, G. Z. Cao and X. G. Zhang, *Adv. Energy. Mater.*, 2013, **3**, 1484-1489.
7. Y. Wang, H. J. Zhang, L. Lu, L. P. Stubbs, C. C. Wong and J. Y. Lin, *ACS Nano*, 2010, **4**, 4753-4761.
8. J. M. Tarascon and M. Armand, *Nature*, 2001, **414**, 359-367.
9. H. Park, T. Song, H. Han, A. Devadoss, J. Yuh, C. Choi and U. Paik, *Electrochem. Commun.*, 2012, **22**, 81-84.
10. Y. Wang, Y. Bai, X. Li, Y. Feng and H. Zhang, *Chemistry*, 2013, **19**, 3340-3347.
11. J. Z. Chen, L. Yang and Y. F. Tang, *J. Power Sources*, 2010, **195**, 6893-6896.
12. B. Wang, J. S. Chen, H. B. Wu, Z. Wang and X. W. Lou, *J. Am. Chem. Soc.*, 2011, **133**, 17146-17148.
13. D. H. Wang, D. W. Choi, J. Li, Z. G. Yang, Z. M. Nie, R. Kou, D. H. Hu, C. M. Wang, L. V. Saraf, J. G. Zhang, I. A. Aksay and J. Liu, *ACS Nano*, 2009, **3**, 907-914.
14. S. J. Park, H. Kim, Y. J. Kim and H. Lee, *Electrochim. Acta*, 2011, **56**, 5355-5362.
15. Z. X. Yang, G. D. Du, Q. Meng, Z. P. Guo, X. B. Yu, Z. X. Chen, T. L. Guo and R. Zeng, *J. Mater. Chem.*, 2012, **22**, 5848-5854.
16. T. Hu, X. Sun, H. T. Sun, M. P. Yu, F. Y. Lu, C. S. Liu and J. Lian, *Carbon*, 2013, **51**, 322-326.
17. B. L. He, B. Dong and H. L. Li, *Electrochem. Commun.*, 2007, **9**, 425-430.
18. C.-C. Tsai and H. Teng, *Chem. Mater.*, 2004, **16**, 4352-4358.
19. Z. H. Bi, M. P. Paranthaman, P. A. Menchhofer, R. R. Dehoff, C. A. Bridges, M. F. Chi, B. K. Guo, X. G. Sun and S. Dai, *J. Power Sources*, 2013, **222**, 461-466.
20. S. Chen, Y. Xin, Y. Zhou, Y. Ma, H. Zhou and L. Qi, *Energy Environ. Sci.*, 2014, **7**, 2597-2603.
21. C. Wang, X. Zhang, Y. Zhang, Y. Jia, J. Yang, P. Sun and Y. Liu, *J. Phys. Chem. C*, 2011, **115**, 22276-22285.
22. H. J. Zhang, Y. Y. Feng, Y. Zhang, L. Fang, W. X. Li, Q. Liu, K. Wu and Y. Wang, *Chemsuschem*, 2014, **7**, 2000-2006.
23. J. Yan, G. Wu, N. Guan, L. Li, Z. Li and X. Cao, *Phys. Chem. Chem. Phys.*, 2013, **15**, 10978.
24. H. J. Zhang, Y. J. Bai, Y. Zhang, X. Li, Y. Y. Feng, Q. Liu, K. Wu and Y. Wang, *Sci. Rep.*, 2013, **3**.
25. S. D. Perera, R. G. Mariano, K. Vu, N. Nour, O. Seitz, Y. Chabal and K. J. Balkus, *Acs Catal.*, 2012, **2**, 949-956.
26. Q. Y. Li and G. X. Lu, *J. Power Sources*, 2008, **185**, 577-583.
27. J.-Y. Liao, H.-P. Lin, H.-Y. Chen, D.-B. Kuang and C.-Y. Su, *J. Mater. Chem.*, 2012, **22**, 1627-1633.

28. G. Kim, C. Jo, W. Kim, J. Chun, S. Yoon, J. Lee and W. Choi, *Energy Environ. Sci.*, 2013, **6**, 2932-2938.
29. J. Zhang, Z. Zhu, Y. Tang, K. Mullen and X. Feng, *Adv. Mater.*, 2014, **26**, 734-738.
30. L. Shen, X. Zhang, H. Li, C. Yuan and G. Cao, *J. Phys. Chem. Lett.*, 2011, **2**, 3096-3101.
31. S. Liu, C. Li, J. Yu and Q. Xiang, *Crystengcomm*, 2011, **13**, 2533-2541.
32. N. Li, G. Liu, C. Zhen, F. Li, L. L. Zhang and H. M. Cheng, *Adv. Funct. Mater.*, 2011, **21**, 1717-1722.
33. L. W. Zhang, H. B. Fu and Y. F. Zhu, *Adv. Funct. Mater.*, 2008, **18**, 2180-2189.
34. Y. Luo, J. Luo, J. Jiang, W. Zhou, H. Yang, X. Qi, H. Zhang, H. J. Fan, D. Y. W. Yu, C. M. Li and T. Yu, *Energy Environ. Sci.*, 2012, **5**, 6559-6566.
35. J. S. Chen, L. A. Archer and X. W. Lou, *J. Mater. Chem.*, 2011, **21**, 9912-9924.
36. J. S. Chen and X. W. Lou, *Electrochem. Commun.*, 2009, **11**, 2332-2335.
37. L. Jin, X. Li, H. Ming, H. Wang, Z. Jia, Y. Fu, J. Adkins, Q. Zhou and J. Zheng, *Rsc Adv.*, 2014, **4**, 6083-6089.
38. D.-H. Lee, J.-G. Park, K. Jin Choi, H.-J. Choi and D.-W. Kim, *Eur. J. Inorg. Chem.*, 2008, **2008**, 878-882.
39. W. Wang, Q. Sa, J. Chen, Y. Wang, H. Jung and Y. Yin, *ACS Appl. Mater. Interfaces*, 2013, **5**, 6478-6483.
40. J. A. Yan, A. Sumboja, E. Khoo and P. S. Lee, *Adv. Mater.*, 2011, **23**, 746-750.
41. T. Xia, W. Zhang, Z. H. Wang, Y. L. Zhang, X. Y. Song, J. Murowchick, V. Battaglia, G. Liu and X. B. Chen, *Nano Energy*, 2014, **6**, 109-118.
42. L. F. He, C. D. Wang, X. L. Yao, R. G. Ma, H. K. Wang, P. R. Chen and K. Zhang, *Carbon*, 2014, **75**, 345-352.
43. P. Y. Chang, C. H. Huang and R. A. Doong, *Carbon*, 2012, **50**, 4259-4268.
44. L. Fang and B. V. R. Chowdari, *J. Power Sources*, 2001, **97-8**, 181-184.
45. J. Qin, C. N. He, N. Q. Zhao, Z. Y. Wang, C. S. Shi, E. Z. Liu and J. J. Li, *ACS Nano*, 2014, **8**, 1728-1738.
46. H. L. Wang, Y. Yang, Y. Y. Liang, J. T. Robinson, Y. G. Li, A. Jackson, Y. Cui and H. J. Dai, *Nano Lett.*, 2011, **11**, 2644-2647.

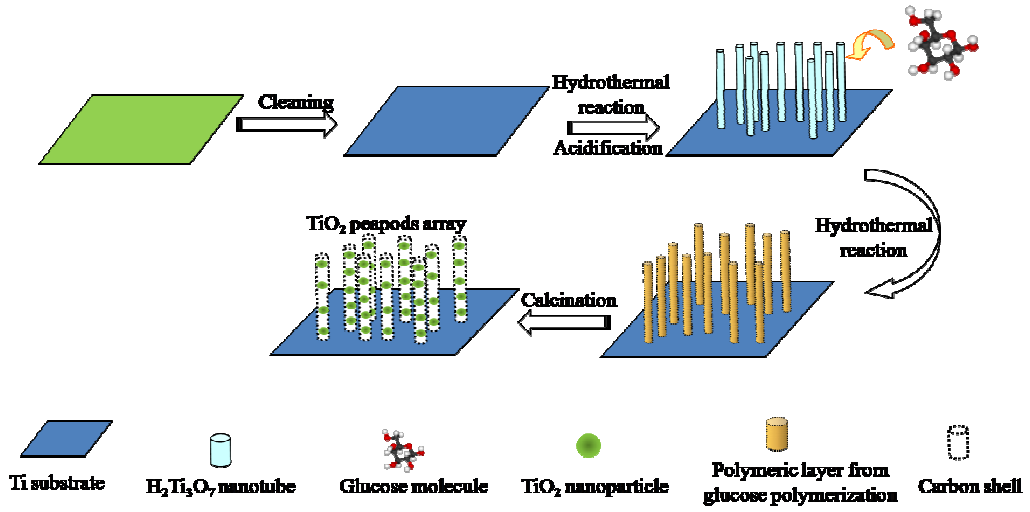

Figure 1. Schematic representation of the fabrication of TiO_2-C peapods array on Ti substrate.

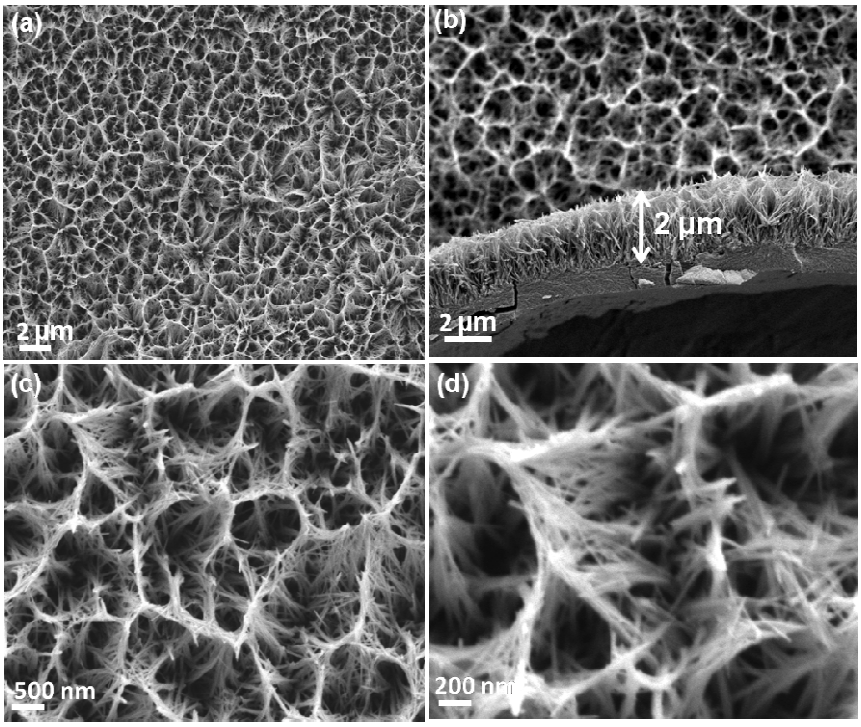

Figure 2. (a and b) Low-magnification SEM images of $H_2Ti_3O_7$ nanotubes array (precursors) on Ti foil. (c and d) High-magnification SEM images of $H_2Ti_3O_7$ nanotubes array, which display these nanotubes upward grown on the substrate.

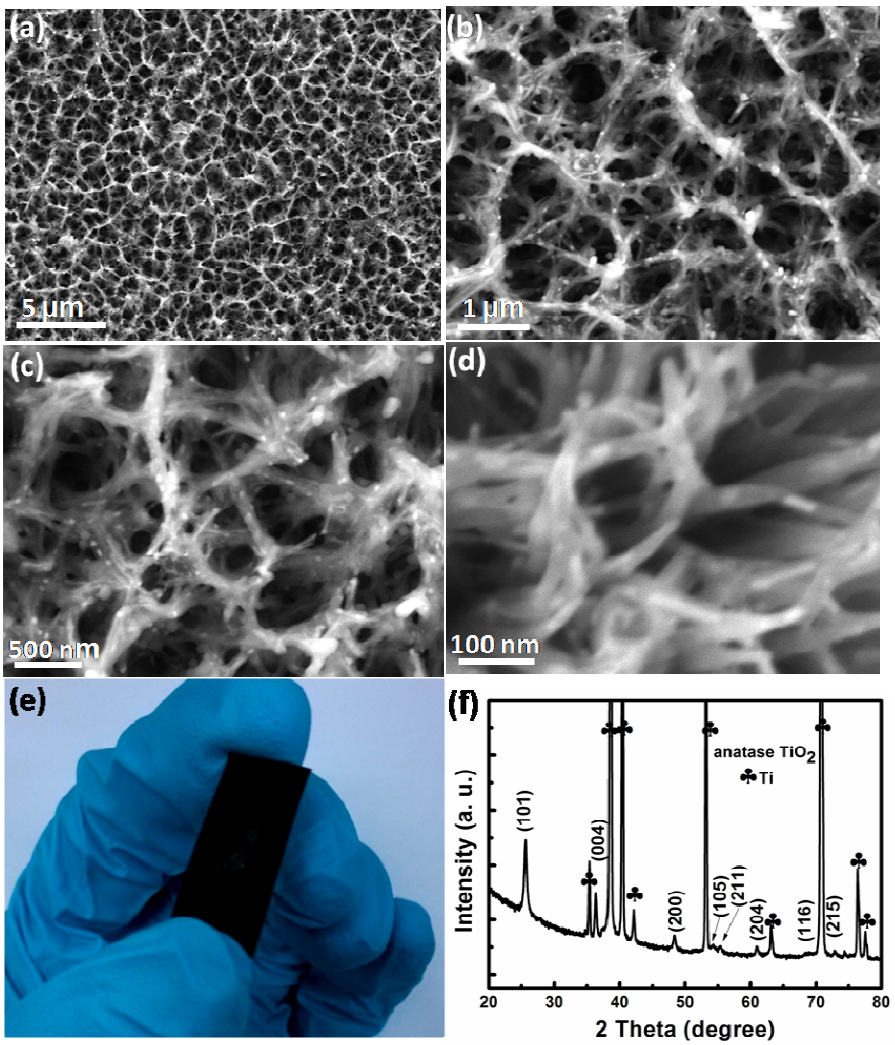

Figure 3. (a and b) Low-magnification SEM images to introduce the uniformity and scalability of TiO_2-C peapods array in a typical synthesis. (c and d) High-magnification SEM images show the specific peapod-like structure. (e) A digital photograph of a self-supported flexible TiO_2-C peapods array electrode. (f) A wide X-ray diffraction angle of 2θ=20-80° proves the pure phase of TiO_2 in the peapods.

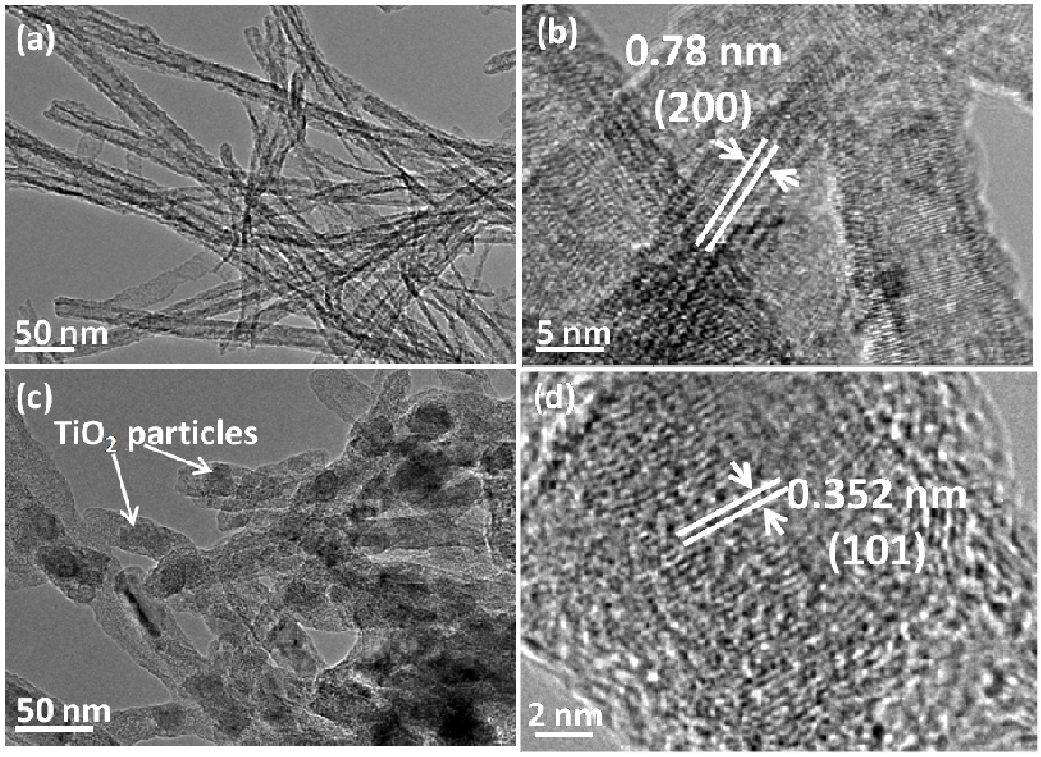

Figure 4. (a) Low-magnification TEM image to confirm the regularity of our precursors. The corresponding HRTEM image (b) indicates the $H_2Ti_3O_7$ nanotubes exhibit well-crystallized features. The ultimately peapod-like TiO2-C array nanocomposite exhibit well-crystallized feature as well (c) and meanwhile form the carbon layers during the annealing in Ar atmosphere (d).

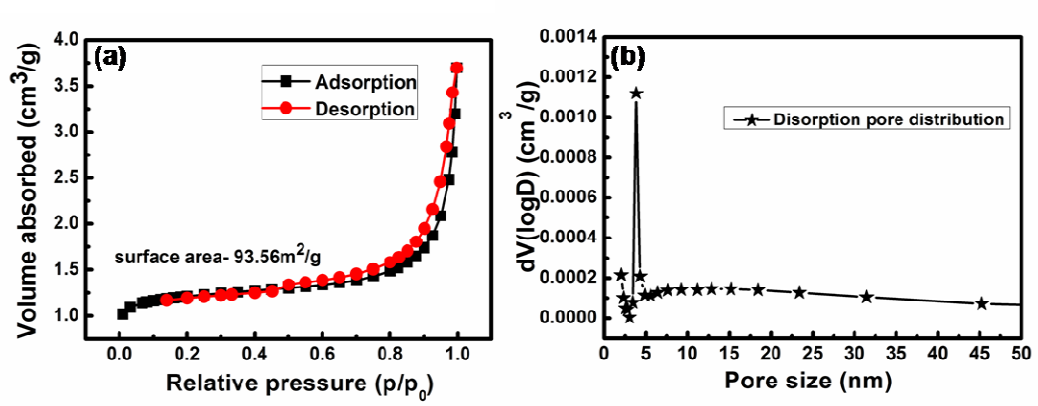

Figure 5. (a) N_2 adsorption-desorption isotherm (BET) diagram of the TiO_2-C peapods array prove the high surface area for our samples. (b) The corresponding pore size distribution of the samples.

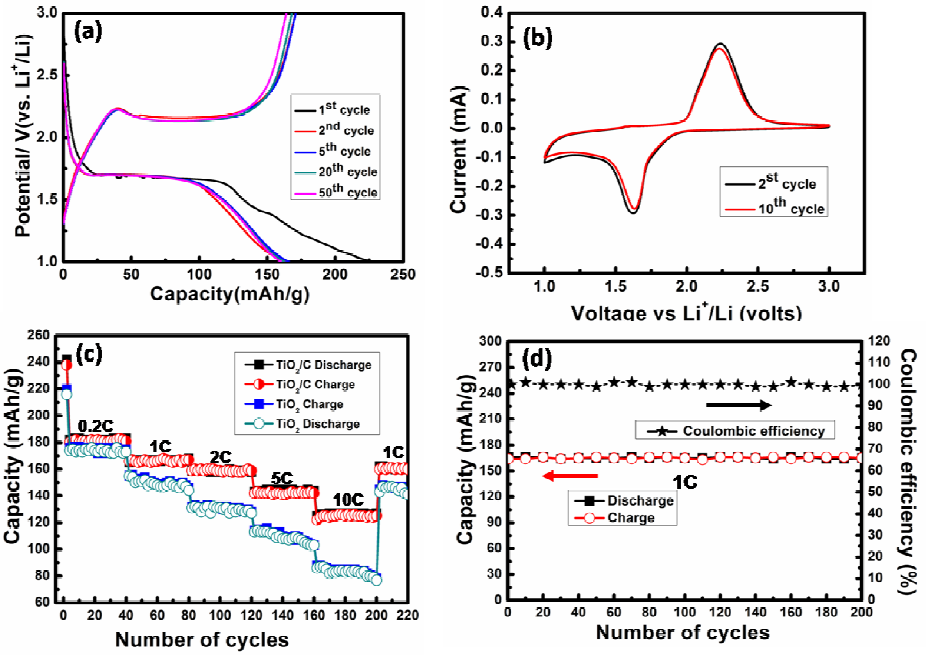

Figure 6. Li-ion storage performances of TiO_2-C peapods array: (a) voltage-capacity curves at 1C; (b) CV curves at a scanning rate of 0.5 mV/s in the voltage range of 1.0-3.0 V; (c) rate capability at different rates (increased 0.2C to 10C); (d) evaluation of coulombic efficiency at a rate of 1C.

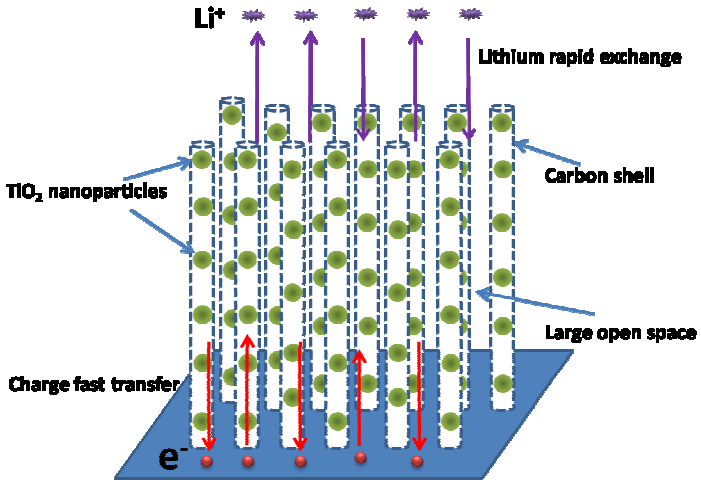

Figure 7. The illustrative mechanism image is presented to systematically reveal the exact reason of the excellent Li storage performance for the TiO_2-C peapods array on Ti foil.